agronomy

MDPI

Article

Evaluation of Spray Performance of Swing-Arm Sprayer on Droplet Deposition on Greenhouse Tomatoes

Zhongyi Yu [1,2], Guangfu Wang [1], Hongtu Zhang [3], Keyao Zhao [1], Xiangsen Meng [3], Jiashu Guo [1], Mingtian Geng [3], Tianze Luo [1], Kekun Zhou [1] and Xiongkui He [1,2,3,*]

[1] College of Science, China Agricultural University, Beijing 100193, China; yuzhongyi6@cau.edu.cn (Z.Y.); Swlskjyxgs@163.com (G.W.); sy20243102460@cau.edu.cn (K.Z.); jiashuguo@cau.edu.cn (J.G.); 2022310060121@cau.edu.cn (T.L.); 2022310060217@cau.edu.cn (K.Z.)
[2] College of Agricultural Unmanned System, China Agricultural University, Beijing 100193, China
[3] College of Engineering, China Agricultural University, Beijing 100083, China; sy20243071752@cau.edu.cn (H.Z.); sy20243071787@cau.edu.cn (X.M.); 17685794429@163.com (M.G.)
* Correspondence: xiongkui@cau.edu.cn

Abstract

In view of the problems existing in the application of greenhouse pesticides in China, this paper developed a swing-arm sprayer for greenhouse high-stem crops through field research and a literature review. Static and dynamic simulations of the swing-arm mechanism were carried out to verify the rationality of the structure. The average contact angle between the water and tomato leaves was 49.39°, while the contact angle of the auxiliary solution on the tomato leaves decreased to 40.98°. An indoor atomization test platform was designed to accurately test the particle size and spray performance. The relative span (RS) of droplet distribution showed that the RS values of nozzles 015, 02, and 03 were relatively small, while the RS value of nozzle 04 was about 1.734. With the addition of additives, the RS value of nozzle 02 decreased from 1.305 to 1.021. The field tests showed that the deposition of fog droplets on the front of tomato leaves was in the order of middle > lower > ground > upper (3.622 μL/cm^2, 3.005 μL/cm^2, 2.977 μL/cm^2, and 2.931 μL/cm^2, respectively). The results indicate that adding additives or increasing the swing-arm angle is beneficial for improving the uniformity of canopy droplet deposition. The front fog droplet coverage of the lower canopy of tomatoes was the lowest, with an average of 26.00%, while the middle and upper canopies had the highest, with an average of 50.58% and 50.72%, respectively. The research found that the spray coverage rate on the front and back sides of tomato leaves was relatively uniform, indicating that the swing-arm greenhouse sprayer designed in this paper could meet the spray quality requirements for tomato pest control.

Keywords: greenhouse chemical control; swing-arm sprayer; droplet deposition distribution; spray performance; parameter optimization; field trial

check for updates

Academic Editor: Jayme Garcia Arnal Barbedo

Received: 1 September 2025
Revised: 17 September 2025
Accepted: 17 September 2025
Published: 19 September 2025

Citation: Yu, Z.; Wang, G.; Zhang, H.; Zhao, K.; Meng, X.; Guo, J.; Geng, M.; Luo, T.; Zhou, K.; He, X. Evaluation of Spray Performance of Swing-Arm Sprayer on Droplet Deposition on Greenhouse Tomatoes. *Agronomy* **2025**, *15*, 2220. https://doi.org/10.3390/agronomy15092220

Copyright: © 2025 by the authors. Licensee MDPI, Basel, Switzerland. This article is an open access article distributed under the terms and conditions of the Creative Commons Attribution (CC BY) license (https://creativecommons.org/licenses/by/4.0/).

1. Introduction

After more than 40 years of rapid development, facility agriculture has not only efficiently saved arable land resources, but has also become a pillar industry for enriching the people, strengthening agriculture, and rural revitalization [1]. In recent years, greenhouse pesticide application technology and equipment have entered a stage of rapid development within the field of agricultural intelligence. Combined with the environmental characteristics of facility agriculture, the development of pesticide application technology has been driven and influenced by multiple factors [2]. On the one hand, population transitions and

labor shortages have exacerbated the problem of "expensive and difficult employment" in greenhouses, making it difficult for people in high-temperature environments to work for long periods of time, greatly restricting the efficiency improvement of greenhouse production [3]. On the other hand, the demand for green, organic, and pesticide residue-free greenhouse agricultural products has continued to grow, and their quality and safety standards have been further improved [4], which has not only improved the efficiency of greenhouse pesticide application but has also alleviated labor shortages, meeting the urgent needs of modern and intelligent facility agriculture [5].

In order to overcome the impact of narrow crop spaces and the complexity of auxiliary facilities on ground autonomous sprayers, Lin et al. [6] researched and developed an autonomous sprayer based on a single-suspension-track air-assisted spray in solar greenhouses, evaluated the spray mode, and conducted laboratory tests to study the airflow distribution and the static spray distribution of the suspender. This independent air-assisted sprayer based on a single suspension track provided a predictable solution for plant protection in solar greenhouses. Li et al. [7] proposed a fixed tube dual fluid mist cooler (FTCF) as a potential solution to address the scarcity of efficient pesticide application equipment for facility cultivation. In order to study the optimal nozzle layout and spray performance, the air flow distribution and spray deposition of FTCF with different nozzle settings were studied through Computational Fluid Dynamics (CFD) simulation experiments. This research provided valuable insights and innovative ideas for strengthening pesticide application technology for protected cultivation. Llop et al. [8] evaluated the impact of air assistance on the application of traditional tomato greenhouse sprays in order to improve the efficacy and efficiency of greenhouse plant protection products. For this reason, three different spray schemes, a handheld trolley sprayer, a self-propelled sprayer, and an autonomous self-propelled sprayer, were evaluated. All the sprays considered were evaluated based on the absolute and normalized canopy deposition, distribution uniformity, and ground loss. It was proved that increasing the air speed does not improve the efficiency of spray application. Nguyen et al. [9] developed an efficient and cost-effective automatic spraying vehicle (ASV) for cherry tomato greenhouses; the key factors of plant growth stage and coverage density when spraying plants in greenhouses have often been overlooked. By using machine vision and the blade density signal of the vertical spray arm to accurately spray, the automation of the entire spraying process was realized, and has the potential to replace the traditional manual spraying method while improving the precision of spraying. At present, the working environment of pesticide application equipment in facility agriculture is confined to small greenhouses, which do not come into contact with crops during operation [10]. Modern greenhouse pesticide application operations have used processes such as manual pesticide application, mechanical pesticide application, automatic pesticide application, and intelligent pesticide application, and can fully achieve autonomous walking, efficient operation, and safe and reliable pesticide application in greenhouses [11]. At present, countries around the world are very enthusiastic about the development potential and application prospects of greenhouse-autonomous, efficient, and precise intelligent pesticide application technology, and are increasing investments in the research and development of a series of intelligent equipment for greenhouse planting and production, such as greenhouse intelligent pesticide application robots. At present, greenhouse pesticide equipment can be divided into four types based on its chassis structure: wheeled, tracked, hybrid, and suspended.

In view of the shortage of pesticide application equipment for existing greenhouse large-scale tall crops, the serious waste associated with traditional greenhouse spraying equipment, and the problem of low target attachment rate, a swing-arm sprayer was designed and developed through testing the different physical and chemical properties of

greenhouse tomato leaves, water, additives, etc. Based on the different types and models of sprinklers, the particle size and spray uniformity of indoor tests were preliminarily screened. Then a field deposition performance test was carried out, by selecting a better combination of operating parameters, to build a chemically efficient control method for greenhouse tomatoes, which will reduce the labor costs and intensity and risks of greenhouse operations, greatly improve the tomato spraying coverage effect, significantly improve the uniformity of greenhouse pesticide spraying, and promote the research and development process of greenhouse plant protection equipment.

2. Materials and Methods

2.1. Study Site, Plant Materials, and Physical Characteristics

After field research and a literature review, it was found that greenhouses in northern China generally adopt single-slope arched structures, which have good insulation and energy-saving effects [12]. The greenhouse tested in this article is located in Pinggu District, Beijing. The greenhouse consists of north and south side walls, an insulated east wall, and a front sloping roof, with a length of about 150 m and a side wall width of 15 m. There is a 1–2 m wide cement walkway under the east wall [13]. The greenhouse tomato planting in this experimental field is mainly a north–south planting mode, with a row spacing of 1 m, a plant spacing of 0.3 m, and a plant height greater than 1.5 m, as shown in Figure 1.

Figure 1. Schematic diagram of northern sunlight greenhouse cultivation for the experiment: 1: main skeleton; 2: greenhouse roof; 3: tomato plant; 4: north wall; 5: side wall; 6: concrete walkway.

The indoor physical and chemical properties tests and spray performance test in this paper were carried out by the laboratory of Chemical Application Technology Center of China Agricultural University in May 2025. Select naturally grown tomatoes were the test materials and we chose the most commonly used chemical additives for testing [14]. We chose the recommended concentration from [15] of Maitu Vegetable Oil Additive (Potential Energy Agricultural Technology (Guangdong) Co., Ltd., Guangzhou, China), and the dosage was 10–20 mL·ha^{-1}.

2.2. Physical Properties Characterization of Spray Liquid

2.2.1. Contact Angle

As shown in the Figure 2a,c. The contact angle of the droplets on the tomato leaves was measured using an optical tensiometer (Attension Theta, Biolin Scientific, Stockholm, Sweden) [16]. The contact angle was recorded five times for each treatment.

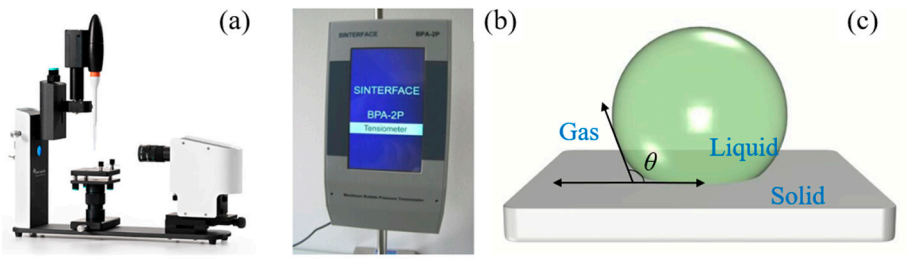

Figure 2. Methods and instruments used for measuring contact angle and surface tension: (**a**) contact angle measuring instrument; (**b**) surface tension meter; (**c**) principle of measuring contact angle.

2.2.2. Surface Tension

The static surface tension of the droplets was also determined using the same optical tensiometer Figure 2b, and the surface tension was measured optically [17]. The liquid was released from a needle, forming a drop hanging from the needle tip. Dynamic surface tension measurements were conducted using a SINTERFACE BPA-2P tensiometer (Sinter face Technologies GmbH, Bad Wildbad, Germany).

2.3. Design of Sprayer and Its Swing-Arm Mechanism

Greenhouse tomato cultivation is mainly close planting and hanging vine planting. The greenhouse space is narrow and it is difficult for machines and tools to enter the ridge for operation [12], in order to achieve the control of tomato diseases and insect pests and determine the effect of pesticide application. Considering the poor application effect of ordinary spraying on the middle and upper canopies of high-stem dry crops, such as tomatoes, combined with the operation action of traditional fruit farmers' manual applications, a swing-arm mechanism for the sprayer is designed independently. Through the swing-arm mechanism, the spray bar is driven to swing up and down, and the spray angle is changed to mimic human-simulated work, so as to improve the effect of spraying [18]. The swing-arm mechanism is mainly used to achieve the up-and-down swinging action of the spray bar. Considering the high operating strength of the swing-arm mechanism to be the most critical part of the spray machine, 45 steel is used in this paper to make it able to withstand large loads and have strong wear resistance. The material density is 7.85 g/cm^3, the yield strength is higher than 355 MPa, its elastic modulus is 196–206 GPa, and its Poisson's ratio is 0.24–0.28. Considering that the swing amplitude of the spray bar is adjusted at around 0.3 m, and the transmission distance between the cam and the eccentric mechanism is relatively short, a larger size is required for implementation. The crank connecting rod mechanism has a simple and reliable structure, low manufacturing cost, strong load-bearing capacity, high transmission efficiency, and can be designed with the required length according to the design needs. Therefore, in this design, the swing-arm structure adopts a crank connecting rod mechanism. The swing-arm mechanism is used to support the spray bar, nozzle, pipeline, and other components, driving the nozzle to swing up and down within a certain range, as shown in Figure 3b. The swing arm adopts a rectangular hollow tube design, which is lightweight, strong, and has good bending and torsion resistance. The material is made of aluminum alloy and polished to reduce contact with the liquid and enhance corrosion resistance. The design is divided into two parts: an upper swing arm and a lower swing arm.

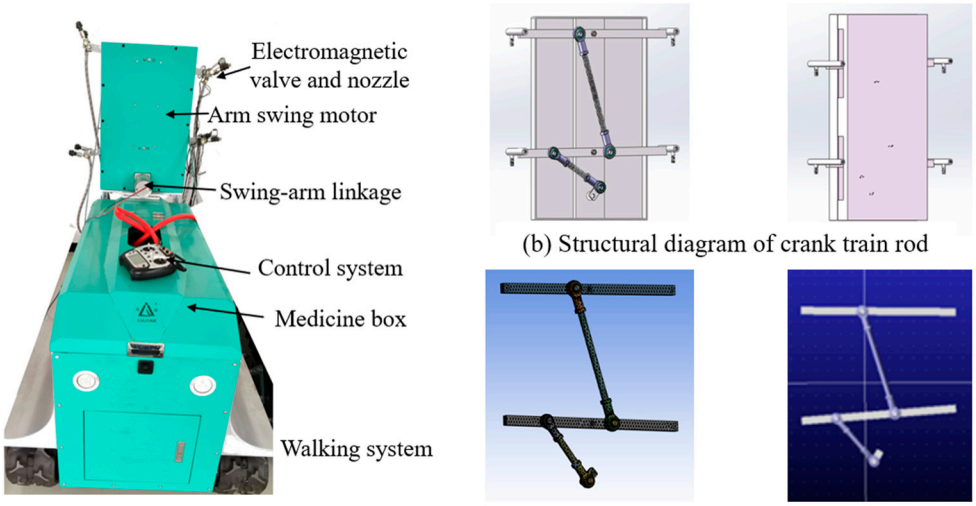

(a) Design of orchard swing-arm sprayer (b) Structural diagram of crank train rod (c) Static simulation mode (d) Dynamic simulation model

Figure 3. Design of the swing-arm spray equipment for greenhouses.

Considering that the strength of each component of the swing-arm structure of the greenhouse sprayer will be damaged during the working process, a static analysis of the swing-arm mechanism is carried out to verify the rationality and safety of the swing-arm structure. We use SOLIDWORKS 2024 (Dassault Systemes, Concord, MA, USA) modeling software to model the swing-arm structure, and then import it into ANSYS 2024 (ANSYS Inc., Pittsburgh, PA, USA) software for a finite element analysis, as shown in Figure 3c. The swing arm and spray bar structure are made of 6061 aluminum alloy material, while the crank and the connecting rod structure are made of high-strength structural steel. A total of 30,968 nodes and 14,514 elements are automatically divided into tetrahedral grids with a grid size of 10 mm. In order to more accurately reflect the stress and strain situation of the swing-arm structure during operation, and to analyze the motion process of the swing-arm structure, dynamic simulation of the swing-arm structure is carried out in ADAMS, as shown in Figure 3c. To accurately establish the kinematic constraint relationship between the components, appropriate motion pair constraints need to be applied based on the actual motion characteristics of the swing-arm mechanism. After reasonably setting the types of constraints, such as the rotating and moving pairs between the components of the swing-arm mechanism, the constraint relationships of the swing-arm mechanism are shown in Figure 4.

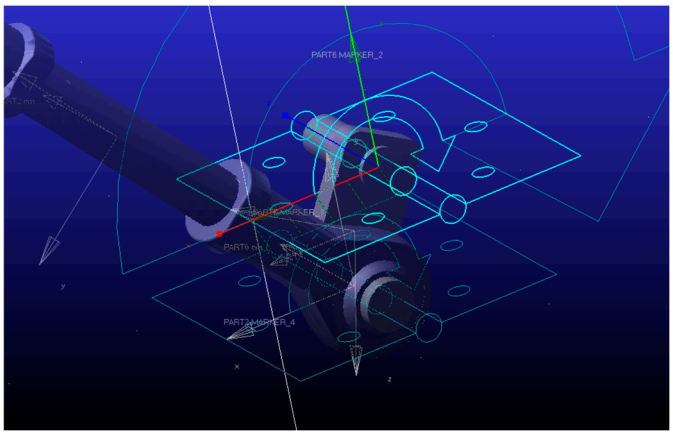

(**a**) Active crank and earth rotating pair.

Figure 4. *Cont.*

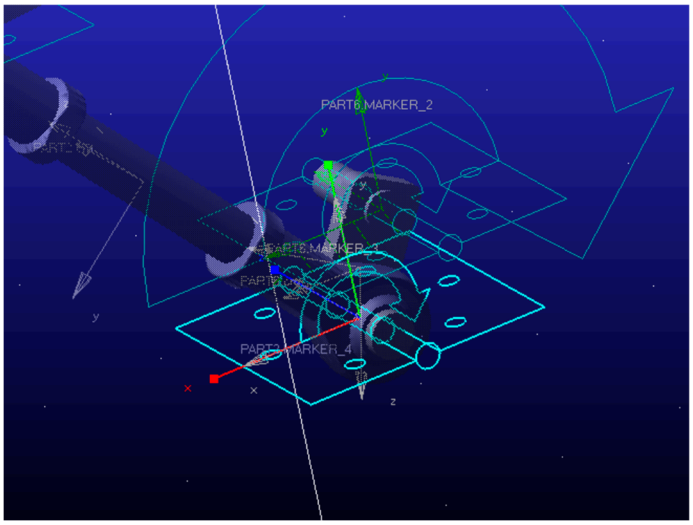

(**b**) Crank and connecting rod rotating pair.

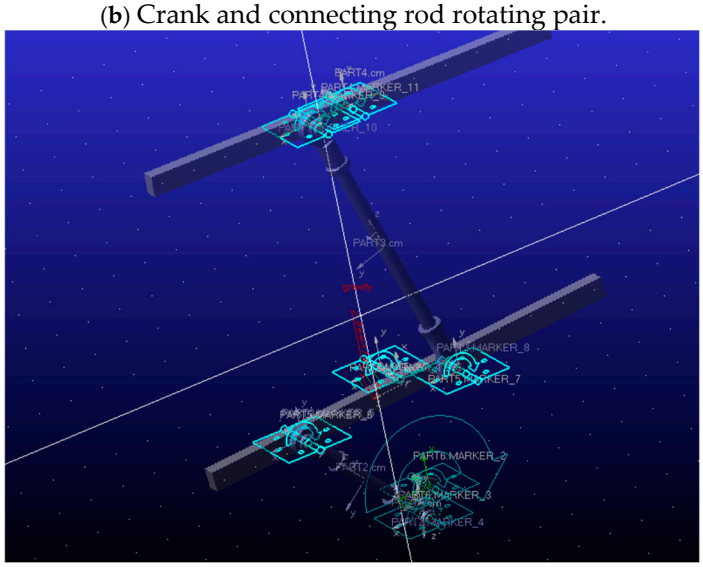

(**c**) Other rotating pairs.

Figure 4. The relationships between the components of the swing-arm mechanism.

2.4. Spray Performance Test

2.4.1. Indoor Spray Performance Test

The droplet size of the XR11002, XR11003, XR110015, TR6004, and TR8002 types of nozzles were tested by a laser particle size analyzer (Spraytec, Malven, Great Malvern, UK) [19]. This study, considering the hazards and pollution of pesticides, uniformly used purified water instead, and set the flow rate of a single nozzle to 1.02 L/min. The relevant parameters and ranges of the test platform are shown in Figure 5, replicating the conditions of subsequent field trials. The parameters, including the $D_{V0.1}$, $D_{V0.5}$, and $D_{V0.9}$ relative spans (RSs) and the spray volume fractions with droplets finer than 100, 150, and 200 µm (V_{100}, V_{150}, V_{200}, and V_{250}), were recorded for analysis [20].

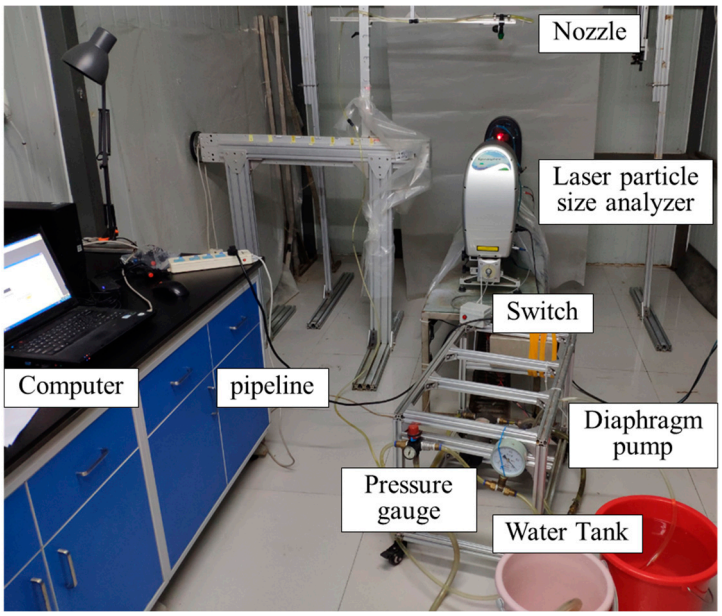

Figure 5. Indoor experimental instrument for droplet size measurement.

2.4.2. Field Trial

To study the optimal performance parameters and operating effects of the greenhouse swing-arm sprayer designed in this study, the standard JB/T 9782-2014 general test method for plant protection machinery was used [21]. We collected the experimental data for pesticide deposition at different positions of greenhouse tomato crops, and analyzed the distribution characteristics of droplet deposition for the system [22]. The filter paper and test cards determined the deposition amount on the tomato leaves based on the light value of dye coloring [23]. In May 2024, field experiments were conducted in tomato greenhouses in Pinggu District, Beijing, China. A tracer, Ponceau 4R (Shanghai Dyestuffs Research Institute Co. Ltd., Shanghai, China), was added to the yellow spray liquid at a concentration of 2 g L^{-1}.

2.5. Experimental Design of Swing-Arm Sprayer on Greenhouse Tomatoes

2.5.1. Sampling Layout

The experimental method is as follows: (1) Determine the sampling points: Select two adjacent tomato plants for each experimental point, and select two experimental points as sampling points for each experiment [24]. (2) Organize test cards and filter paper: Each sampling point is subjected to positive and negative sampling, with a total of 24 filter papers and 24 test cards for each experiment, located in the upper, middle, and lower layers of the tomato tree crown. The ground part is collected in a culture dish [25], with 4 samples per experiment (Figure 6). (3) According to the experimental scheme, the field tomato application experiment using the swing-arm sprayer is carried out. (4) Collect samples: Filter paper is used to measure the spray deposition on the tomatoes at different canopy positions, and test cards are used to measure the coverage. (5) Result processing: Use DepositScan software to analyze the scanned test card images, determine coverage, and calculate the coefficient of variation. Use a microplate reader (diluted 20 times) to optically analyze the deposition amount of droplet distribution on filter paper.

Figure 6. Layout of the sprayer sample collection in each treatment area.

2.5.2. Treatment Design

In order to better study the influence of operating parameters on the spray effect, the forward speed of greenhouse swing-arm sprayer was set to 1 m/s, and the spray pressure was set to 1 MPa. According to the previous pre-experiment results, the rotation speed of the swing-arm mechanism is the most appropriate when it is 60 r/min. A group of static spray operation controls were set, and the spray angles were 0°, −45°, and 45°. Through a large number of previous indoor spray and high-speed camera pre-experiments, the nozzle performance under different flow rates was determined and, combined with the actual situation of the spray machine, a single nozzle flow rate of 1.02 L/min was finally selected. The application parameters of these on-site experiments are shown in Table 1.

Table 1. Primary application parameters of the field tests in 2025.

Treatment	Nozzle Model	Spray Angle (°)	Swing-Arm Rotation Speed (r/min)	Swing-Arm Angle (°)	Forward Speed (m/s)
F1	XR11002	110	0	0	1
F2	XR11002	110	60	0	1
F3	XR11002	110	60	45	1
F4	XR11002	110	60	−45	1
F5	XR11003	110	60	45	1
F6	TR8002	80	60	45	1
F7	TR6004	60	60	45	1
F8	TR8002-A	110	60	45	1

2.6. Treatment of Test Results

2.6.1. Evaluation Metrics

After treatment, ImageJ 1.53k software (National Institutes of Health, Bethesda, MD, USA) was employed to extract the data on the spray coverage (%) from the scanned images. The atomization performance was evaluated by the droplet size distribution. According to ISO (International Organization for Standardization) standard 24253-2 [26,27], the deposition was be calculated using the following Equation (1):

$$\beta_{\text{dep}} = \frac{(\rho_{smpl} - \rho_{blk}) \times F_{cal} \times V_{dii}}{\rho_{spray} \times A_{col}} \tag{1}$$

where β_{dep} is the spray deposition, μL cm^{-2}; ρ_{smpl} is the tracer reading; ρ_{blk} is the tracer reading of the blanks (dilution water); F_{cal} is the calibration factor; V_{dii} is the volume of dilution liquid for the tracer from the collector, L; ρ_{spray} is the spray concentration, or

amount of tracer solute in the spray liquid sampled at the nozzle, g L^{-1}; and A_{col} is the projected area of the collector for capturing the spray deposition, cm^2.

2.6.2. Statistical Analyses

The data were analyzed using Origin 2024 (EA Company, Redwood City, CA, USA) [28]. In all instances, the mean values for the spray deposition, droplet size, droplet density, spray coverage, and spray performance were compared using Duncan's post hoc test at a significance level of 0.05.

3. Results and Discussion

3.1. Physical Properties

The dynamic surface tension of spray liquid is shown in Figure 7a. The average value of water and auxiliary solution was 73.55 and 68.05 mN m^{-1}, respectively. However, enhancing the wetting time of the pesticide improved the spreading performance and adhesion of droplets on the tomato surfaces [29].

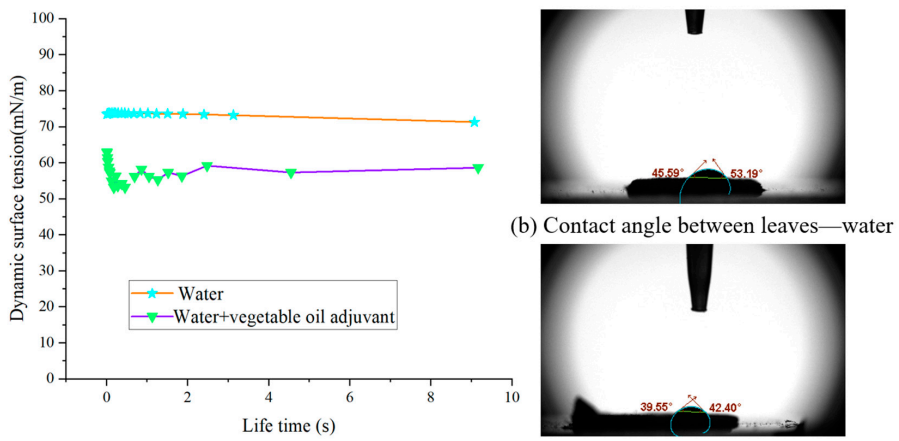

(a) Dynamic surface tension (b) Contact angle between leaves—water (c) Contact angle between leaves—adjuvant

Figure 7. Measurement of physical properties of spray solutions.

The results regarding the contact angles are shown in Figure 7b,c. The average contact angle between the water and tomato leaves was 49.39°, while the contact angle of the auxiliary solution on the tomato leaves decreased to 40.98°. This indicates that the addition of additives to the liquid reduces the contact angle on the tomato leaves.

3.2. Static and Dynamic Simulations of Swing-Arm Mechanism

Through static simulation of the swing-arm structure, it was found that the maximum total deformation occurs at the end of the lower swing arm, and the maximum equivalent elastic strain and stress occur at the connection between the lower swing arm and the short rocker arm. The maximum equivalent elastic strain was 5.45×10^{-2}, and the maximum equivalent stress was 86.15 MPa, which were within the yield strength of the material (Figure 8).

By analyzing the angular velocity curves of each rotating pair, it was found that rotating pair 2, which is between the crank and the short rocker, has the highest angular velocity, with a higher risk factor than the other rotating pairs, but within the yield strength of the material. From the angular velocity curves of each rotating pair, it can be seen that the angular velocity of each rotating pair cycles within a certain period, and the peak value is in the middle and late stages of one cycle. The acceleration peak of rotating pair 1, which is the one connected to the crankshaft and motor, is the highest and experiences significant impact fluctuations. Therefore, attention was paid to its strength in the subsequent testing process (Figure 9).

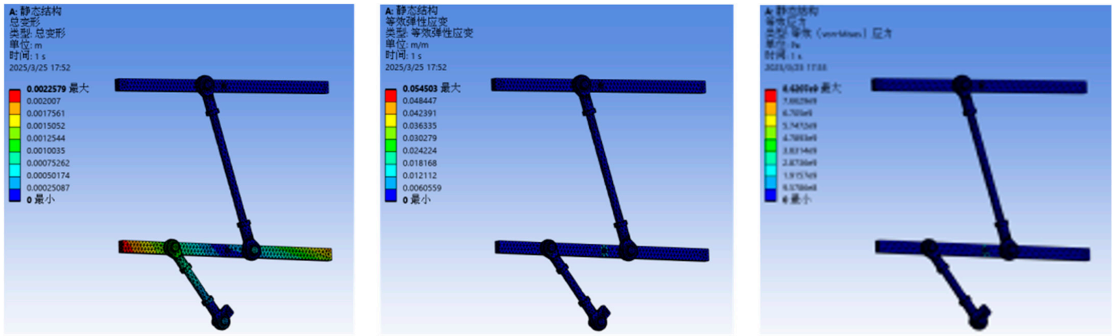

(a) Total deformation diagram (b) Equivalent elastic strain diagram (c) Equivalent stress diagram

Figure 8. Static simulation result diagram of swing-arm mechanism.

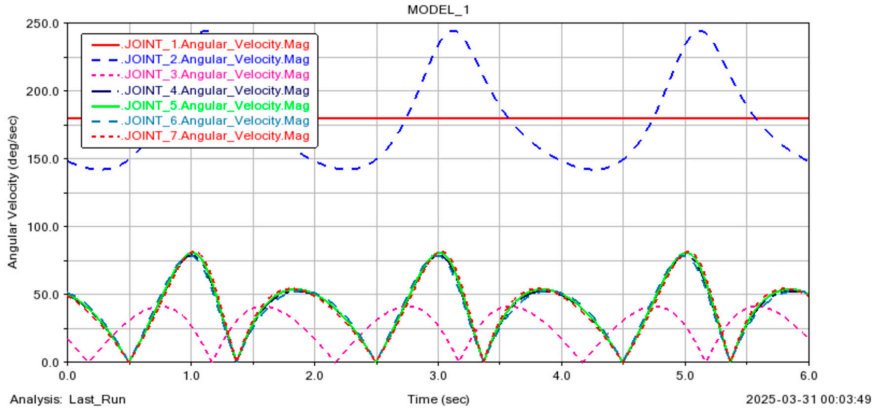

(**a**) Angular velocity curves of each rotating pair.

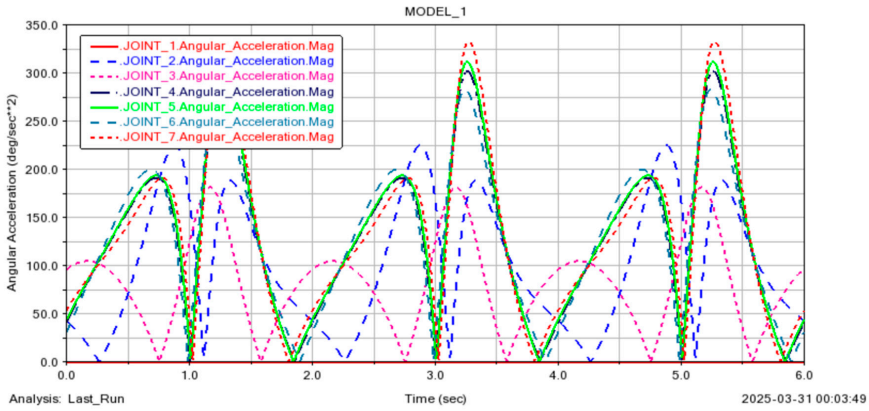

(**b**) Acceleration curves of each rotating pair.

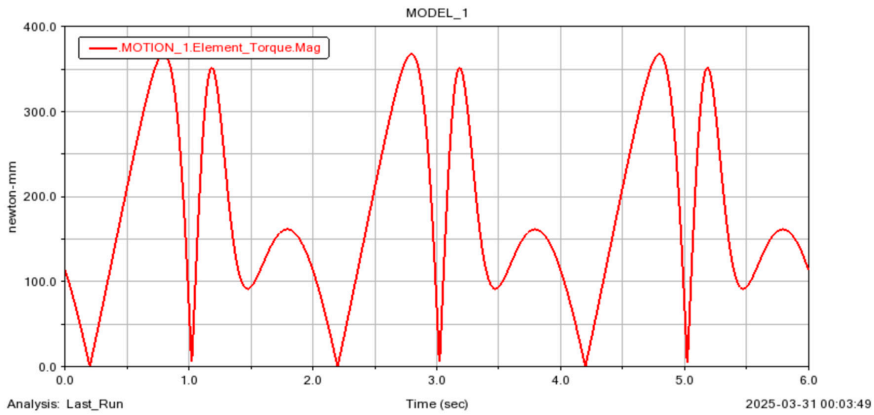

(**c**) Torque curve of the driving pair.

Figure 9. Dynamics simulation result curves of swing-arm mechanism.

3.3. Droplet Size Distribution and Spray Effect

The droplet size spectrum of spray solution using an indoor spray platform [30] are shown in Table 2 and Figure 10. According to the JB/T9782-2014 standard [31], under the same stable pressure, nozzle models 015 and 02 produced small droplets, while nozzles 03 and 04 produced medium-sized droplets, with little difference in their numerical values. Adding an auxiliary solution slightly increased the particle size, but the RS value was smaller and more stable [27]. The relative span (RS) of droplet distribution shows that the RS values of nozzles 015, 02, and 03 were relatively small, while the RS value of nozzle 04 was about 1.734, which was the highest. Adding additives reduced the RS value. With the addition of additives, the RS value of nozzle 02 decreased from 1.305 to 1.021.

Table 2. Droplet size spectrum of spray solutions using fixed-pipeline high-pressure spray platform.

Nozzle	Droplet Size Spectrum of the Fixed-Pipeline High-Pressure Spray Platform							
	$D_{V0.1}$ (μm)	$D_{V0.5}$ (μm)	$D_{V0.9}$ (μm)	V_{100} (%)	V_{150} (%)	V_{200} (%)	V_{250} (%)	RS
XR11002	78.61	138.7	231	22.59	57.33	81.42	93.48	1.099
XR11003	91.79	165.5	307.6	13.86	41.87	65.18	80.17	1.304
XR110015	84.39	142.9	243.5	19.59	54.54	78.75	91.11	1.113
TR6004	78.53	170.7	374.5	18.95	41.69	60.06	72.99	1.734
TR8002	55.9	118.1	210.1	37.27	69	87.66	96.12	1.305
TR8002-A	78.48	130.5	211.8	25.14	63.83	86.86	96.35	1.021

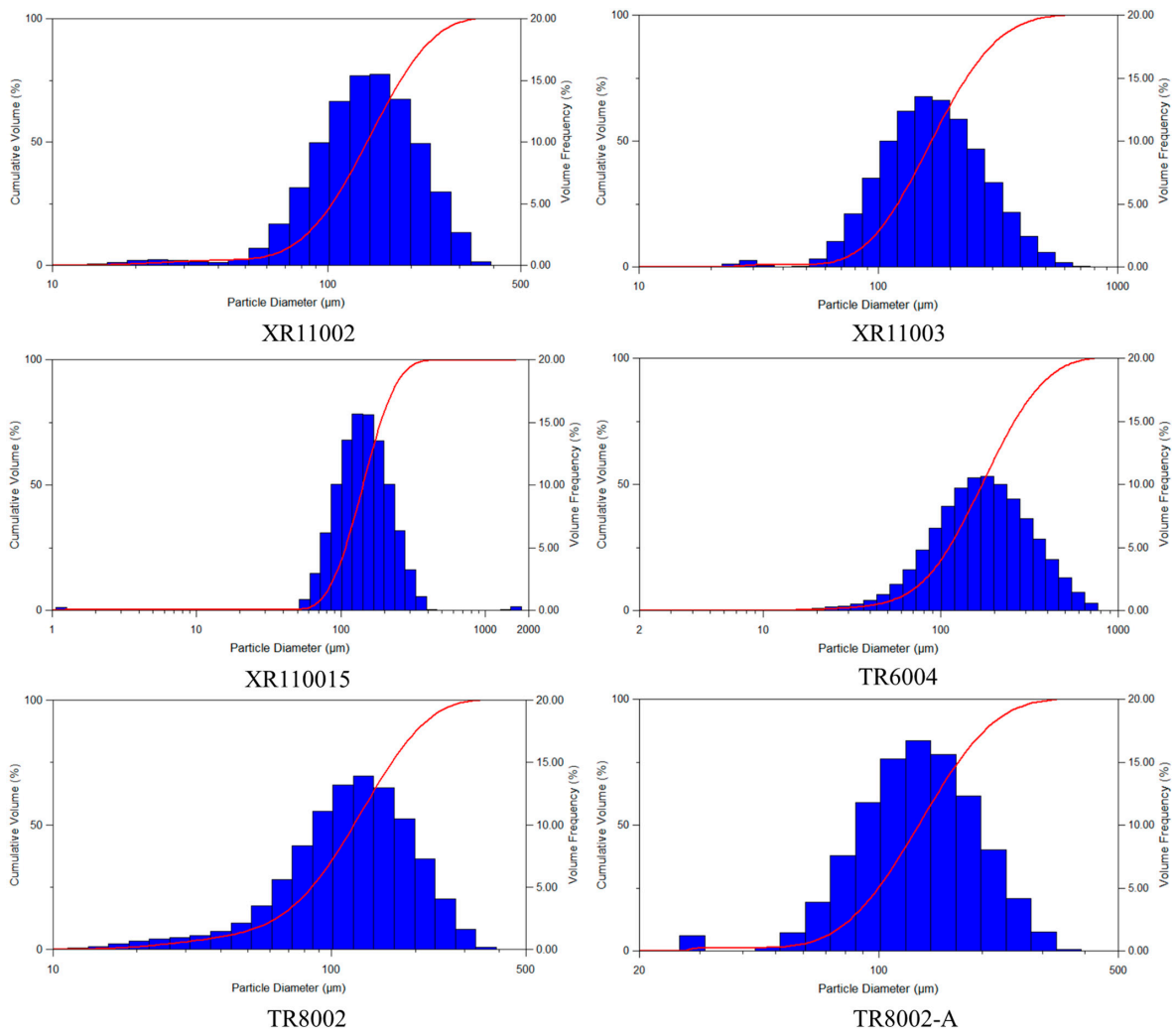

Figure 10. Particle size distribution curve of each test nozzle.

The swing-arm sprayer designed in this paper is an innovative design, and the shapes and models of related nozzles are difficult to determine. Therefore, an indoor high-speed camera spray performance test platform was built [30]. By testing five nozzles with different shapes and models under the same pressure (0.1 MPa), the sprayers with the best performance were preliminarily selected according to their atomization effects, and used for the subsequent field experiments to reduce the test burden. The spray effect is shown in Figure 11. The fog shape of the fan-shaped nozzle XR110015 was too dispersed, and it was easy for the fine-sized particles size to spread and drift away. The fog shape of nozzles XR11002 and XR11003 was relatively concentrated, and the coverage was relatively wide. The three-dimensional coverage of the conical nozzles TR8002 and TR6004 was more extensive, the overall spray effect performance was also better, and the spray effect after adding additives was better.

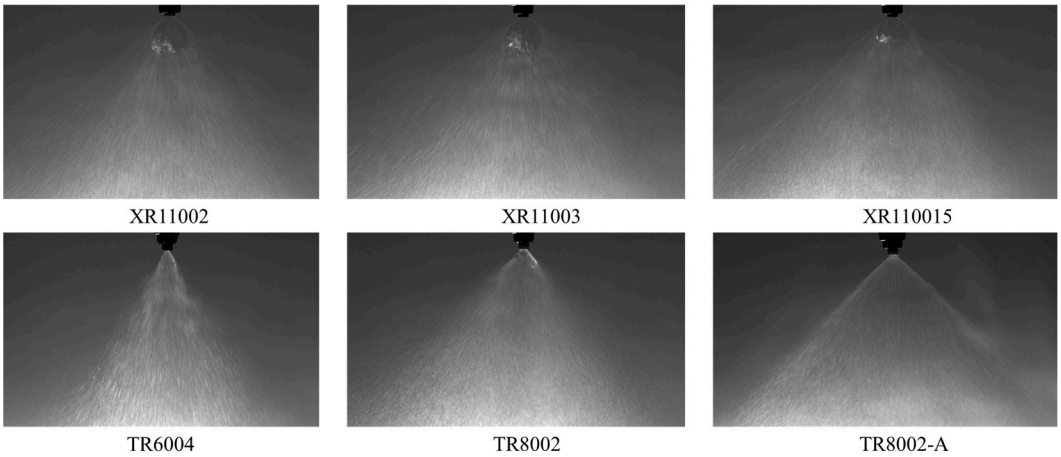

Figure 11. Spray performance diagram of each test nozzle.

3.4. Application Results to Tomatoes in Greenhouses

3.4.1. Spray Deposition

The solution used for indoor testing in this article was water and the yellow dye used in the field, and the liquid flow rate of a single nozzle was 1.02 L/min. The distance between the nozzle and the target surface in the indoor and field experiments was about 0.5 m. According to the deposition amount of fog droplets on the front of leaves at the different canopy positions of tomatoes (Figure 12), the deposition amount followed the order middle > lower > ground > upper (3.622 μL/cm^2, 3.005 μL/cm^2, 2.977 μL/cm^2, and 2.931 μL/cm^2, respectively). Comparing the effects of eight field trials, it can be seen that the F2, F3, and F8 groups had the highest sedimentation amounts in the three parts of the canopy, with total amounts of 14.688 μL/cm^2, 11.624 μL/cm^2, and 10.962 μL/cm^2, respectively, which was significantly higher than that of F6 and F7 groups (6.375 μL/cm^2 and 7.500 μL/cm^2). It is speculated that the reason for this may be due to an insufficient swing-arm operation, resulting in insufficient adhesion to the upper canopy leaves of tomatoes, and more droplets being transported to the middle and lower canopies. The results indicate that adding additives or increasing the swing-arm angle is beneficial for improving the uniformity of canopy droplet deposition.

The deposition amount on the back of the leaves was lower than that on the front of the leaves (Figure 13). In all positions of the canopy [32], the deposition amount of F8 group was the highest. The deposition of fog droplets on the back of tomato leaves followed the order lower > upper > middle (1.918 μL/cm^2, 1.555 μL/cm^2, and 1.467 μL/cm^2, respectively). The deposition amount of F8 on the upper, middle, and lower parts of the canopy was 2.100 μL/cm^2, 1.526 μL/cm^2, and 2.507 μL/cm^2, respectively. The total deposition of F8

on the canopy was higher than that of other groups, indicating that adding additives is beneficial for increasing the droplet deposition on leaf backs. Considering that there was less deposition on the back of the lower canopy, this may have been due to the insufficient swing-arm amplitude of the swing-arm mechanism for the lower part, similar to the direct deposition of droplets from top to bottom in a closed greenhouse environment.

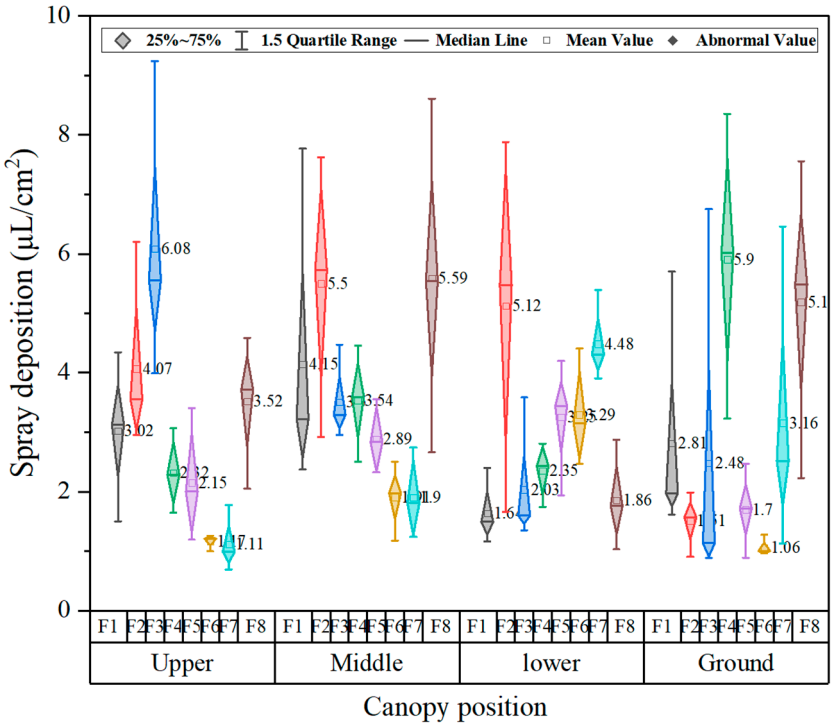

Figure 12. Droplet deposition on the front of leaves.

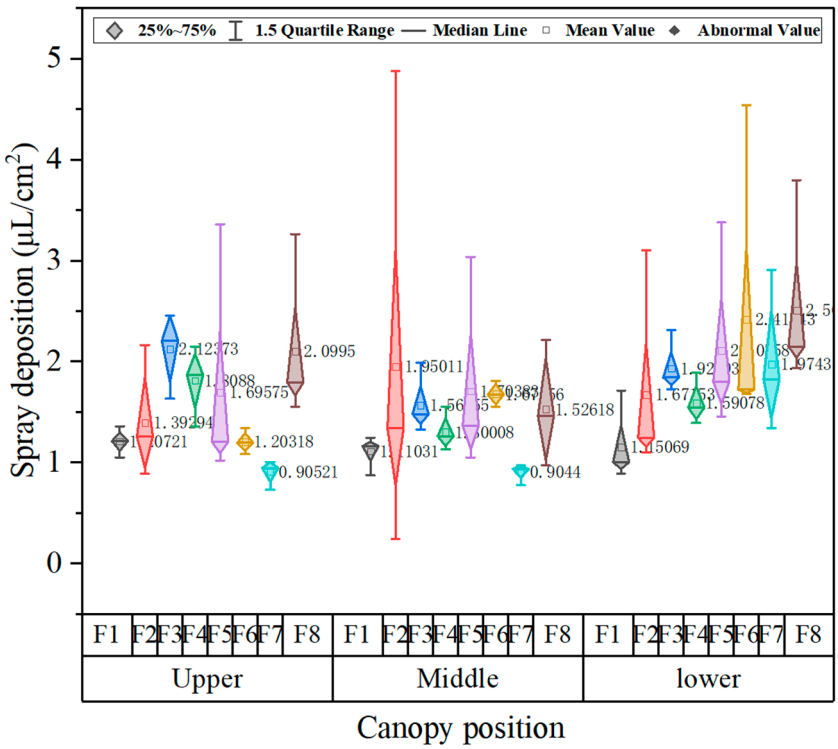

Figure 13. Droplet deposition on the back of leaves.

3.4.2. Spray Coverage Rate

The results of the analysis using the digital image analysis software Image (Maryland, USA) [19] are shown in Figures 14 and 15. (1) Under the same spray particle size and swing-arm speed, compared with the spray angles (45°, −45°) of F3 and F4 groups, the average positive and negative coverage rate of tomato canopy leaves by the F2 group was 51.15% and 20.07%, respectively, higher than the 31.37% and the 11.07% of F3 group, and higher than the 46.99% and 9.87% of F4 group, which was likely to lead to more deposition and loss of droplets. (2) Under the same swing-arm speed and spray angle, the positive and negative coverage rate of tomato leaves by the F7 group was higher than those of F6 group. The positive and negative coverage rate of tomato leaves by the F3 group was higher than those of the F6 group, which showed that the spray effects of different sprinkler models were also different, and the spray performance of nozzles 03 and 04 was better than that of nozzle 02. (3) Compared with the F3 and F5 groups, under the same operating parameters, the larger the spray particle size, the better the coverage rate, and the performance of sprinkler 03 was better than that of sprinkler 02. (4) Compared with the F6 and F7 groups, under the same operating parameters, the larger the spray particle size, the better the coverage rate, and the performance of 04 nozzle was better than that of 02 nozzle.

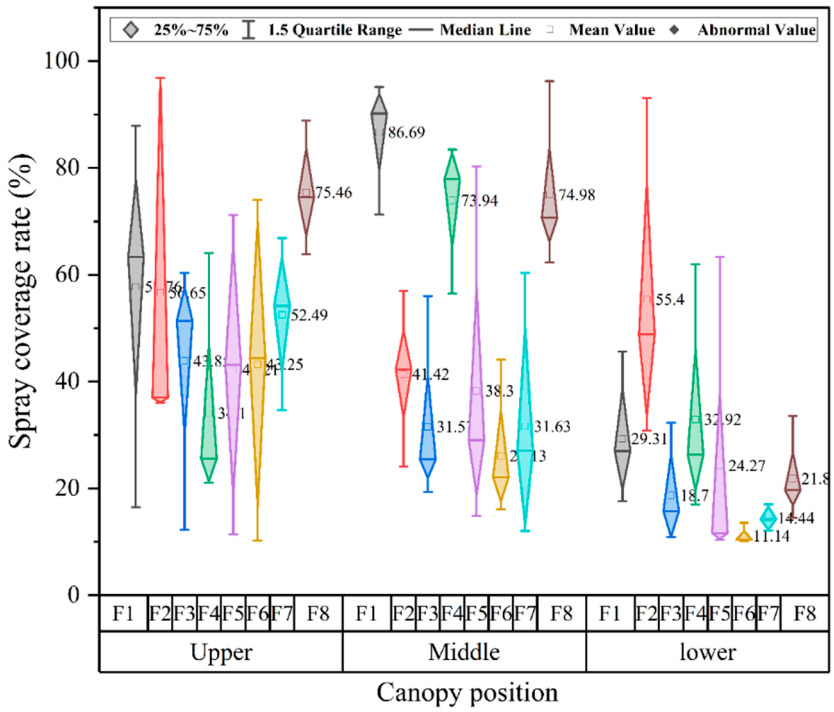

Figure 14. Spray coverage rate of upper, middle, and lower canopy leaves' fronts.

Compared with the spray angle, the swing-arm speed, and nozzle model, the average coverage rate of each tomato canopy fluctuated greatly, so the spray uniformity effect was general. From Figures 14 and 15, it can be seen that the front fog droplet coverage of the lower canopy of tomatoes was the lowest, with an average of 26.00%, while the middle and upper canopies were the highest, with an average of 50.58% and 50.72%, respectively. The overall uniformity of the back coverage was good, which can effectively protect. On the back of tomato leaves. The research found that the spray coverage rate on the front and back sides of tomato leaves was relatively uniform, indicating that the swing-arm greenhouse sprayer designed in this paper can meet the spray quality requirements for tomato pest control.

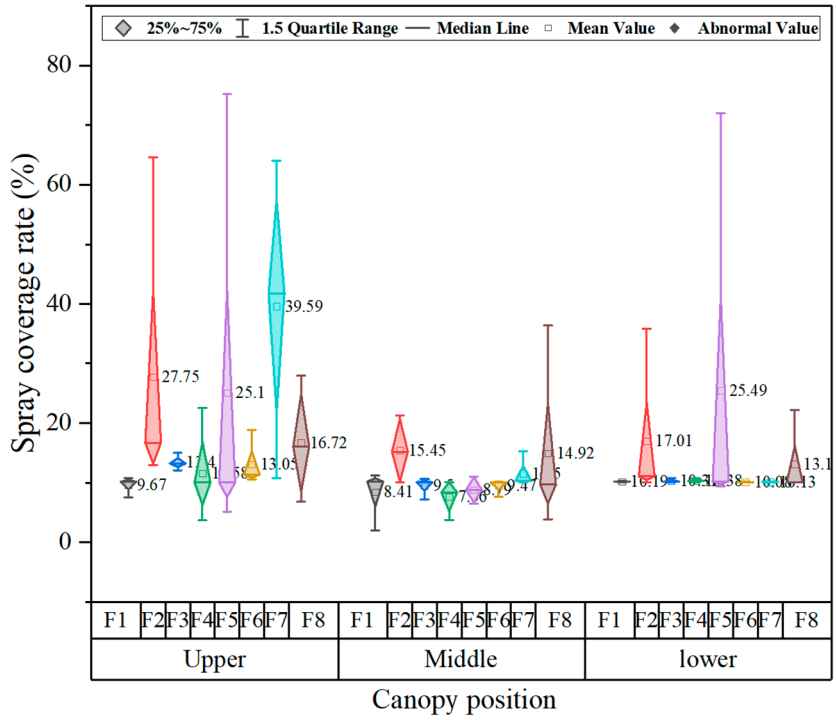

Figure 15. Spray coverage rate of upper, middle, and lower canopy leaves' backs.

4. Conclusions

In view of the problems existing in the application of greenhouse pesticides in China, this study developed a swing-arm sprayer for greenhouse high-stem crops through field research and a literature review, and carried out indoor physical and chemical properties tests, spray particle size and atomization performance tests combined with experimental aids, carried out a structural simulation of the swing-arm mechanism in terms of statics and dynamics, and finally carried out a greenhouse field performance test, and studied the atomization effect, operating efficiency, deposition, and loss characteristics. The main content is as follows:

(1) A swing-arm-type greenhouse sprayer was developed for greenhouse crops, such as tomatoes. Static and dynamic simulations of the swing-arm mechanism, a key component, were carried out to verify the rationality of the structure.

(2) The average values of water and auxiliary solution were 73.55 and 68.05 mN m^{-1}, respectively. The average contact angle between the water and tomato leaves was 49.39°, while the contact angle of the auxiliary solution on the tomato leaves decreased to 40.98°. This indicates that the addition of additives to the liquid reduces the contact angle on the tomato leaves.

(3) An indoor atomization test platform was designed to accurately test the particle size and spray performance. By testing five nozzles with different shapes and models under the same pressure, the sprayers with the best performance were preliminarily selected according to their atomization effects, and used for the subsequent field experiments to reduce the test burden. Adding an auxiliary solution slightly increased the particle size, but the RS value was smaller and more stable. The relative span (RS) of droplet distribution showed that the RS values of nozzles 015, 02, and 03 were relatively small, while the RS value of nozzle 04 was about 1.734, which was the highest. Adding additives can reduce the RS value. With the addition of additives, the RS value of nozzle 02 decreased from 1.305 to 1.021.

(4) The field tests showed that the deposition of fog droplets on the front of tomato leaves followed the order middle > lower > ground > upper (3.622 μL/cm^2, 3.005 μL/cm^2, 2.977 μL/cm^2, and 2.931 μL/cm^2, respectively). Comparing the effects of eight field trials, it could be seen that the F2, F3, and F8 groups had the highest sedimentation amounts in the three parts of the canopy, with total amounts of 14.688 μL/cm^2, 11.624 μL/cm^2, and 10.962 μL/cm^2, respectively, which were significantly higher than those of F6 and F7 groups (6.375 μL/cm^2 and 7.500 μL/cm^2). The results indicate that adding additives or increasing the swing-arm angle is beneficial for improving the uniformity of canopy droplet deposition. Compared with the spray angle, the swing-arm speed, and nozzle model, the average coverage rate of each tomato canopy fluctuated greatly, so the spray uniformity effect was general. From Figures 14 and 15, it can be seen that the front fog droplet coverage of the lower canopy of tomatoes was the lowest, with an average of 26.00%, while the middle and upper canopies were the highest, with an average of 50.58% and 50.72%, respectively. The overall uniformity of the back coverage was good, which can effectively solve the problem of adhesion on the back of tomato leaves. The research found that the spray coverage rate on the front and back sides of tomato leaves was relatively uniform, indicating that the swing-arm greenhouse spray designed in this paper can meet the spray quality requirements for tomato pest control.

Author Contributions: Conceptualization, X.H. and H.Z.; methodology, X.H., K.Z. (Keyao Zhao), and Z.Y.; analysis, X.M. and G.W.; investigation, J.G. and Z.Y.; resources, X.H., J.G., M.G. and Z.Y.; data curation, T.L. and Z.Y.; writing—original draft preparation, Z.Y.; writing—review and editing, X.H. and Z.Y.; visualization, Z.Y.; supervision, K.Z. (Kekun Zhou); project administration, X.H.; funding acquisition, X.H. All authors have read and agreed to the published version of the manuscript.

Funding: This study was funded by the earmarked fund for China Agriculture Research System (No. CARS-28), the 2115 Talent Development Program of China Agricultural University (No. 2115-89052), and the Natural Science Foundation of China (No. 31761133019).

Data Availability Statement: The original contributions presented in the study are included in the article, further inquiries can be directed to the corresponding author.

Acknowledgments: The authors would like to thank all other staff of CCAT and CAUS, China Agricultural University, Zhejiang Longhao Agriculture and Forestry Technology Co., Ltd., and the Plant Protection Station, Beijing, for their great contributions to this work.

Conflicts of Interest: The authors declare no conflicts of interest.

References

1. Zhang, D.; Huang, Y.; Wu, C.; Ma, M. Detecting tomato disease types and degrees using multi-branch and destruction learning. *Comput. Electron. Agric.* **2023**, *213*, 108244. [CrossRef]
2. Yan, T.; Zhu, H.; Sun, L.; Wang, X.; Ling, P. Detection of 3-D objects with a 2-D laser scanning sensor for greenhouse spray applications. *Comput. Electron. Agric.* **2018**, *152*, 363–374. [CrossRef]
3. Ma, J.; Xiang, S.; Shi, Y.; Xie, X.; Chai, A.; Li, L.; Li, B.; Fan, T. Application of ultra-low-volume spray for the control of vegetable disease in greenhouse: Investigation of formulation performance and potential dermal exposure. *Pest Manag. Sci.* **2024**, *80*, 2761–2772.
4. Fu, Q.; Li, X.; Zhang, G.; Ma, Y. Improved greenhouse self-propelled precision spraying machine—Multiple height and level (MHL) control. *Comput. Electron. Agric.* **2022**, *201*, 107265. [CrossRef]
5. Rincón, V.J.; Grella, M.; Marucco, P.; Alcatro, L.E.; Balsari, P. Spray performance assessment of a remote-controlled vehicle prototype for pesticide application in greenhouse tomato crops. *Sci. Total Environ.* **2020**, *726*, 138509. [CrossRef] [PubMed]
6. Lin, J.; Ma, J.; Liu, K.; Huang, X.; Xiao, L.; Ahmed, S.; Dong, X.; Qiu, B. Development and test of an autonomous air-assisted sprayer based on single hanging track for solar greenhouse. *Crop Prot.* **2021**, *142*, 105502. [CrossRef]

7. Li, X.; Nuyttens, D.; Xu, T.; Jin, Z.; Wang, S.; Lv, X. Spray performance simulation and experiment analysis of a greenhouse fixed-pipe twin-fluid cold fogger with different nozzle settings. *Pest Manag. Sci.* **2024**, *80*, 17. [CrossRef]
8. Llop, J.; Gil, E.; Llorens, J.; Gallart, M.; Balsari, P. Influence of air-assistance on spray application for tomato plants in greenhouses. *Crop Prot.* **2015**, *78*, 293–301. [CrossRef]
9. Nguyen, N.T.A.; Pham, C.C.; Lin, W.C. Development of a line following autonomous spraying vehicle with Machine vision-based leaf density estimation for cherry tomato greenhouses. *Comput. Electron. Agric.* **2023**, *215*, 13. [CrossRef]
10. Sánchez-Hermosilla, J.; Rincón, V.J.; Páez, F.; Fernández, M. Comparative spray deposits by manually pulled trolley sprayer and a spray gun in greenhouse tomato crops. *Crop Prot.* **2011**, *31*, 119–124. [CrossRef]
11. Sanji, S.M.; Jafari, M.; Masoumi, A. Development and evaluation of a rope climbing sprayer robot for greenhouse environment. *Crop Prot.* **2024**, *182*, 106749. [CrossRef]
12. He, L.; Ding, L.; Waterhouse, G.I.; Li, B.; Liu, F.; Li, P. Performance matching between the surface structure of cucumber powdery mildew in different growth stages and the properties of surfactant solution. *Pest Manag. Sci.* **2021**, *77*, 3538–3546. [CrossRef]
13. Lin, B.; Song, H.; Liu, G.; Qi, Z.; Guan, R.; Wei, M.; Zhang, G.; Jia, Y.; Wang, S. In-situ testing and analysis of aerodynamic characteristics of tomato plants in large-span arched greenhouse. *Comput. Electron. Agric.* **2025**, *230*, 109891. [CrossRef]
14. Hewitt, A.J. Adjuvant use for the management of pesticide drift, leaching and runoff. *Pest. Manag. Sci.* **2024**, *80*, 4819–4827. [CrossRef] [PubMed]
15. Holloway, P.J.; Ellis, M.C.B.; Webb, D.A.; Western, N.M.; Tuck, C.R.; Hayes, A.L.; Miller, P.C.H. Effects of some agricultural tank-mix adjuvants on the deposition efficiency of aqueous sprays on foliage. *Crop Prot.* **2000**, *19*, 27–37. [CrossRef]
16. Zhang, C.; Liu, R.; Liu, K.; Yang, X.; Liu, H.; Diao, M.; Li, M. A CFD transient model of leaf wetness duration on greenhouse cucumber leaves. *Comput. Electron. Agric.* **2022**, *200*, 107257. [CrossRef]
17. Nairn, J.J.; Alison, F.W. Importance of adjuvant formulation properties in predicting wetting on leaf surfaces. *Pest Manag. Sci.* **2022**, *80*, 212–219. [CrossRef] [PubMed]
18. Salas, B.; Salcedo, R.; Garcia-Ruiz, F.G.E. Design, implementation and validation of a sensor-based precise airblast sprayer to improve pesticide applications in orchards. *Precis. Agric.* **2024**, *25*, 865–888. [CrossRef]
19. Ryszard, H.; Grzegorz, D.; Waldemar, Z.; Paweł, K.; Artur, G. Effect of Nozzle Type and Adjuvants on Spray Coverage on Apple Leaves. *Agronomy* **2021**, *11*, 1790. [CrossRef]
20. Liu, S.; Zhang, X.; Wang, X.; Feng, R.; Wu, J.; Zhang, S.; Xu, J. Vibration inducing and airflow guiding coupled tomato pollination method research based on gas–solid two-phase flow model. *Comput. Electron. Agric.* **2024**, *216*, 108472. [CrossRef]
21. Huang, C.; Zhang, X.; Chen, J.; Lv, S.; Ma, L. Equipment for crop protection: Standardization development in China. *Agric. Eng. Int. CIGR E-J.* **2011**, *13*, 1–6.
22. Grella, M.; Gioelli, F.; Marucco, P.; Zwertvaegher, I.; Mozzanini, E.; Mylonas, N.; Nuyttens, D.; Balsari, P. Field assessment of a pulse width modulation (PWM) spray system applying different spray volumes: Duty cycle and forward speed effects on vines spray coverage. *Precis. Agric.* **2021**, *23*, 219–252. [CrossRef]
23. Yu, S.; Cui, L.; Cui, H.; Liu, X.; Liu, J.; Xin, Z.; Yuan, J.; Wang, D. Spray performance of flexible shield canopy opener and rotor wind integrated boom sprayer application in soybean: Effects on droplet deposition distribution. *Pest Manag. Sci.* **2024**, *80*, 3334–3348. [CrossRef] [PubMed]
24. Kang, C.; He, L.; Zhu, H. Assessment of spray patterns and efficiency of an unmanned sprayer used in planar growing systems. *Precis. Agric.* **2024**, *25*, 2271–2291. [CrossRef]
25. Michael, C.; Gil, E.; Gallart, M.; Stavrinides, M.C. Influence of Spray Technology and Application Rate on Leaf Deposit and Ground Losses in Mountain Viticulture. *Agriculture* **2020**, *10*, 615. [CrossRef]
26. Liu, Z.; Chen, J.; Guo, J.; Qiu, B. Numerical Simulation and Validation of Droplet Deposition on Tomato Leaf Surface under Air-Assisted Spraying. *Agronomy* **2024**, *14*, 1661. [CrossRef]
27. Wongsuk, S.; Zhu, Z.; Zheng, A.; Qi, P.; Li, Y.; Huang, Z.; Han, H.; Wang, C.; He, X. Assessing the potential spray drift of a six-rotor unmanned aerial vehicle sprayer using a test bench and airborne drift collectors under low wind velocities: Impact of atomization characteristics and application parameters. *Pest Manag. Sci.* **2024**, *80*, 6053–6067. [CrossRef]
28. Saiful, H.A.; Xiongzhe, H.; SeungHwa, Y. Independent Control Spraying System for UAV-Based Precise Variable Sprayer: A Review. *Drones* **2022**, *6*, 383. [CrossRef]
29. He, L.; Ding, L.; Zhang, P.; Li, B.; Mu, W.; Liu, F. Impact of the equilibrium relationship between deposition and wettability behavior on the high-efficiency utilization of pesticides. *Pest Manag. Sci.* **2021**, *77*, 2485–2493. [CrossRef]
30. Zhang, R.; Hu, P.; Li, L.; Tang, Q.; Yang, J.; Yang, J.; Chen, L. Fine-grained method for determining size and velocity distribution patterns of flat-fan nozzle-atomised droplets based on phase doppler interferometer. *Comput. Electron. Agric.* **2024**, *225*, 109343. [CrossRef]

31. *JB/T 9782-2014*; Equipment for Crop Protection—General Test Methods. Ministry of Industry and Information Technology of the People's Republic of China: Beijing, China, 2014.
32. Zhu, T.; Ma, X.; Guan, H.; Wu, X.; Wang, F.; Yang, C.; Jiang, Q. A calculation method of phenotypic traits based on three-dimensional reconstruction of tomato canopy. *Comput. Electron. Agric.* **2023**, *204*, 107515. [CrossRef]

Disclaimer/Publisher's Note: The statements, opinions and data contained in all publications are solely those of the individual author(s) and contributor(s) and not of MDPI and/or the editor(s). MDPI and/or the editor(s) disclaim responsibility for any injury to people or property resulting from any ideas, methods, instructions or products referred to in the content.